The 2013 World Congress on
Advances in Structural Engineering and Mechanics (ASEM13)
Jeju, Korea, September 8-12, 2013

Effects of thickness variations on the thermal elastoplastic behavior of annular discs

*Yun-Che Wang[1)], Sergei Alexandrov[2,3)] and Yeau-Ren Jeng[3)]

[1)] *Department of Civil Engineering, National Cheng Kung University, Tainan 70101, Taiwan*
[2)] *A. Ishlinskii Institute for Problems in Mechanics, Russian Academy of Sciences, 119526 Moscow, Russia*
[3)] *Department of Mechanical Engineering and Advanced Institute of Manufacturing with High-tech Innovations, National Chung Cheng University, 62102 Chia-Yi, Taiwan*
[1)] yunche@mail.ncku.edu.tw

ABSTRACT

Metallic annular discs with their outer boundary fully constrained are studied with newly derived semi-analytical solutions for the effects of thickness variations under thermal loading and unloading. The plane stress and axisymmetric assumptions were adopted, and the thickness of the disk depends on the radius hyperbolically with an exponent *n*. Furthermore, it is assumed that the stress state is two dimensional and temperature is uniform in the domain. The solutions include the elastic, elastic-plastic and plastic-collapse behavior, depending on the values of temperature. The von Mises type yield criterion is adopted in this work. The material properties, Young's modulus, yield stress and thermal expansion coefficient, are assumed temperature dependent, while the Poisson's ratio is assumed to be temperature independent. It is found that for any *n* values, if the normalized hole radius *a* greater than 0.6, the normalized temperature difference between the elastically reversible temperature and plastic collapse temperature is a monotonically decreasing function of inner radius. For small holes, the *n* values have strong effects on the normalized temperature difference. Furthermore, it is shown that thickness variations may have stronger effects on the strain distributions when temperature-dependent material properties are considered.

1. INTRODUCTION

A metallic thin disk under thermal loading and unloading is of particular importance in engineering design. Under cycling loading, residual stress may

[1)] Associate Professor
[2,3)] Professor
Note: Copied from the manuscript submitted to "Structural Engineering and Mechanics, An International Journal" for presentation at ASEM13 Congress

accumulated in the material, causing pre-mature failure (Withers 2007). Continuum level modeling requires a choice of constitutive relationships. Various plasticity models have been proposed, and they can be viewed as plasticity theorems with different definition of internal variables (Horstemeyer and Bammann 2010). Popular models, such as the Tresca and von Mises yield criterion, are widely adopted in the theoretical and numerical studies to model the mechanical behavior of materials beyond elasticity. In this work, we adopt the von Mises yield criterion for its superiority in modeling metal plasticity.

In the literature, Thompson and Lester (1946) studied the stress in rotating disks under high temperatures. Vivio and Vullo (2010) studied residual stresses in rotating disk having the hyperbolic profile has been studied for estimating its service life under overspeeding. In addition, the thermal yield of a rotating hyperbolic disk is discussed (Alujevic et al. 1993). The elastic-plastic stress analyses have been conducted in rotating disks without considerations of elevated temperature and thickness variations (You and Zhang 1999, Rees 1999, Gamer 1984). Furthermore, Lenard and Haddow (1972) the plastic collapse of rotating cylinders with the plain strain assumption. Alexandrov et al. (2012) studied residual stresses and pressure dependence on the yield criterion in a thin disk. In addition, anisotropic effects in rotating disk have been analyzed with inclusions of plastic deformation (Alexandrova and Alexandrov 2004). As a closely related research area, Zimmerman and Lutz (1999) studied the thermal stresses in functionally graded material have been studied under uniform heating.

Most aforementioned studies in the past do not consider material properties depending on temperature. Temperature-dependent material properties are important in analyzing the thermal stresses in materials (Noda 1991, Argeso and Eraslan 2008). Neglect of the effects of material properties being functions of temperature may lead to catastrophic failures in engineering. Eraslan studied the rotating disk with rigid inclusion and nonlinear hardening variable thickness has been studied for its plastic stresses with von Mises yield criterion. With similar ideas, the disk under external pressure has been analyzed (Eraslan et al. 2005). In addition, solid disks under concave profiles under rotation have been investigated (Eraslan and Orcan 2002). Furthermore, Eraslan has investigated annular disks with various boundary conditions under rotations. In addition to annular disks, elastic-plastic stress in a disk containing a rigid inclusion has been analyzed (Guven 1998).

Theoretical developments in the annular disk problem under various loading and boundary conditions with different material models have long been conducted to better predict the mechanical behavior of the disk. However, most of the approaches in the literature do not provide analytical solutions for the combined effects of temperature-dependent material properties and thickness variations. Hence, in this work, analytical solutions, that include the temperature dependent material properties and hyperbolic thickness profiles, are derived under the plane stress assumption with the von Mises type yield criterion. The exact solutions developed here may be of use in benchmark tests for future numerical studies.

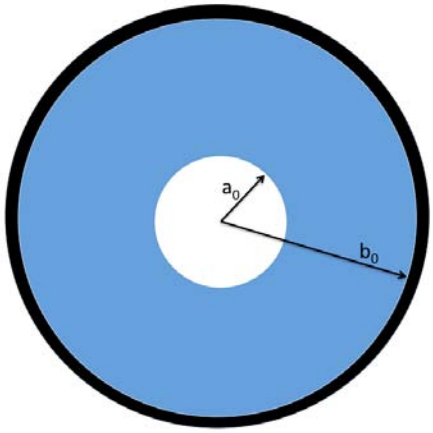

Figure 1. Schematic of the annular disk (blue) with the inner radius a_0 and outer radius b_0, fully constrained at the outer boundary (thick black).

2. THEORETICAL

In this section, the preliminary setup of the mathematical derivation is described in Section 2.1. Subsequently, Section 2.2 contains the elastic solution, Section 2.3 the elastic/plastic stress solution, and Section 2.4 the elastic/plastic strain solution. Finally, in Section 2.4, solutions for fully plastic deformation are presented at high temperatures.

2.1 Mathematical setup

It is assumed that the initial thickness (before loading) of the disk varies according to the equation

$$h = h_0\left(\frac{r}{a_0}\right)^n \tag{1}$$

where h_0 is the thickness at the inner rim, r = a_0, and h the thickness at the outer rim, r = b_0, of the thin hollow elastic-plastic disc, as schematically shown in Figure 1. The disc is inserted into a rigid container of radius b_0, which provides complete displacement confinement, and subjected to thermal loading by an uniform temperature field throughout the disc. The exponent n is a parameter to control the thickness profile of the disc. A graphical demonstration of the effects of the exponent n, with respect to normalized radius = r/a_0, is shown in Figure 2. It can be seen that for n = 0 the disc has a uniform thickness everywhere. For n > 0, the thickness close to the disc center is smaller, and vice versa.

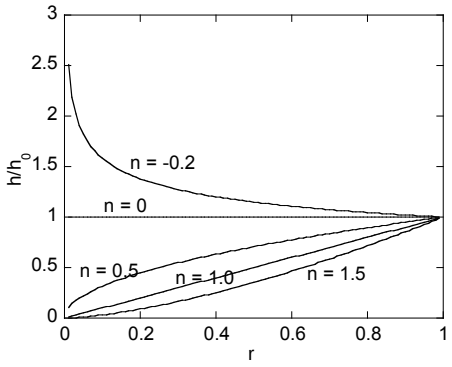

Figure 2. Thickness profile calculated from Eq. (1).

The disc has no stress at the initial instant. The increase in temperature from its initial value, *T*, and the constraints imposed on the disc affects the zero stress state. It is natural to introduce a cylindrical coordinate system (r, θ, z) with its *z*- axis coinciding with the axis of symmetry of the disc. Symmetry dictates that the normal stresses in this coordinate system, σ_r, σ_θ and σ_z, are the principal stresses and the circumferential displacement vanishes everywhere. The radial displacement is denoted by *u*. It is supposed that the state of stress is plane ($\sigma_z = 0$) and the strains are small. Plastic yielding is controlled by the Mises yield criterion. In the case under consideration this criterion can be written as

$$\sigma_r^2 + \sigma_\theta^2 - \sigma_\theta \sigma_r = \sigma_Y^2 \tag{2}$$

where σ_Y is the yield stress in uniaxial tension. The classical Duhamel-Neumann law is adopted. In particular, the elastic portions of the total strains are related to the stresses as

$$\varepsilon_r^e = \frac{\sigma_r - \nu\sigma_\theta}{E}, \quad \varepsilon_\theta^e = \frac{\sigma_\theta - \nu\sigma_r}{E}, \quad \varepsilon_z^e = -\frac{\nu(\sigma_r + \sigma_\theta)}{E} \tag{3}$$

where *E* is Young's modulus and ν is Poisson's ratio. The thermal portions of the total strains are given by

$$\varepsilon_r^T = \varepsilon_\theta^T = \varepsilon_z^T = \gamma T \tag{4}$$

where γ is the thermal coefficient of linear expansion. The total strains in plastic regions are

$$\varepsilon_r = \varepsilon_r^T + \varepsilon_r^e + \varepsilon_r^p, \quad \varepsilon_\theta = \varepsilon_\theta^T + \varepsilon_\theta^e + \varepsilon_\theta^p, \quad \varepsilon_z = \varepsilon_z^T + \varepsilon_z^e + \varepsilon_z^p \tag{5}$$

where $\varepsilon_r^p, \varepsilon_\theta^p$ and ε_z^p are the plastic portions of the total strains. In the case under consideration, the total radial and circumferential strains are

$$\varepsilon_r = \frac{\partial u}{\partial r}, \quad \varepsilon_\theta = \frac{u}{r}. \tag{6}$$

The flow theory of plasticity is adopted. Therefore, the associated flow rule connects stresses and strain rates rather than strains. Since the strains are small, the components of the strain rate tensor are obtained as the local time derivatives of the corresponding components of the strain tensor. However, since the material model is rate-independent, these time derivatives can be replaced with the corresponding

derivatives with respect to any other monotonically increasing parameter. Denote this parameter by *p*. Then,

$$\begin{aligned}
&\zeta_r = \frac{\partial \varepsilon_r}{\partial p}, \quad \zeta_\theta = \frac{\partial \varepsilon_\theta}{\partial p}, \quad \zeta_z = \frac{\partial \varepsilon_z}{\partial p}, \\
&\zeta_r^e = \frac{\partial \varepsilon_r^e}{\partial p}, \quad \zeta_\theta^e = \frac{\partial \varepsilon_\theta^e}{\partial p}, \quad \zeta_z^e = \frac{\partial \varepsilon_z^e}{\partial p}, \\
&\zeta_r^p = \frac{\partial \varepsilon_r^p}{\partial p}, \quad \zeta_\theta^p = \frac{\partial \varepsilon_\theta^p}{\partial p}, \quad \zeta_z^p = \frac{\partial \varepsilon_z^p}{\partial p}.
\end{aligned} \tag{7}$$

The associated flow rule gives

$$\zeta_r^p = \lambda\left(2\sigma_r - \sigma_\theta\right), \quad \zeta_\theta^p = \lambda\left(2\sigma_\theta - \sigma_r\right), \quad \zeta_z^p = -\lambda\left(\sigma_r + \sigma_\theta\right) \tag{8}$$

where $\lambda \geq 0$. It is supposed that σ_Y, E and γ are dependent of temperature whereas ν is not. Time-independent Poisson's ratio is a reasonable assumption for many materials (Noda 1991). The temperature-dependent properties are represented as

$$E = E_0 f_E(T), \quad \gamma = \gamma_0 f_\gamma(T), \quad \sigma_Y = \sigma_0 f_\sigma(T) \tag{9}$$

where E_0, γ_0, and σ_0 are constants whereas $f_E(T)$, $f_\gamma(T)$, and $f_\sigma(T)$ are prescribed functions of *T*. With no loss of generality, it is possible to put $f_E(0) = f_\gamma(0) = f_\sigma(0) = 1$.

It is convenient to introduce the following dimensionless quantities

$$\rho = \frac{r}{b_0} \quad \text{and} \quad a = \frac{a_0}{b_0}. \tag{10}$$

Using (1) the only non-trivial equilibrium equation is

$$\rho \frac{\partial \sigma_r}{\partial \rho} + (1+n)\sigma_r = \sigma_\theta \tag{11}$$

The boundary conditions are

$$\sigma_r = 0 \tag{12}$$

for $\rho = a$ and $u = 0$ for $\rho = 1$. It is evident from (6) that the latter is equivalent to

$$\varepsilon_\theta = 0 \tag{13}$$

for $\rho = 1$.

2.2 Elastic solution

In the following, the elastic solution and the initiation of plastic yielding are developed. In the case of axisymmetric plane stress problems the general thermo-elastic solution is

$$\frac{\sigma_r}{\sigma_Y} = A\rho^{\gamma_1} + B\rho^{\gamma_2}, \quad \frac{\sigma_\theta}{\sigma_Y} = A(1+n+\gamma_1)\rho^{\gamma_1} + B(1+n+\gamma_2)\rho^{\gamma_2} \tag{14}$$

$$\frac{\varepsilon_r}{k} = A\left[1-\left(1+n+\gamma_1\right)\nu\right]\rho^{\gamma_1} + B\left[1-\left(1+n+\gamma_2\right)\nu\right]\rho^{\gamma_2} + \tau,$$
$$\frac{\varepsilon_\theta}{k} = A\left(1+n-\nu+\gamma_1\right)\rho^{\gamma_1} + B\left(1+n-\nu+\gamma_2\right)\rho^{\gamma_2} + \tau, \tag{15}$$
$$\frac{\varepsilon_z}{k} = -\nu\left[A\left(2+n+\gamma_1\right)\rho^{\gamma_1} + B\left(2+n+\gamma_2\right)\rho^{\gamma_2}\right] + \tau.$$

where *A* and *B* are constants of integration and

$$k = \frac{\sigma_Y}{E}, \quad t = \frac{gT}{k},$$
$$g_1 = -\left(1+\frac{n}{2}\right) - \frac{1}{2}\sqrt{\left(2-n\right)^2 + 4n\left(1-n\right)}, \tag{16}$$
$$g_2 = -\left(1+\frac{n}{2}\right) + \frac{1}{2}\sqrt{\left(2-n\right)^2 + 4n\left(1-n\right)}$$

When the entire disc is elastic, *A* and *B* are determined from (12) and (13) as

$$A = A_e = -\frac{\tau a^{\gamma_2}}{\left(1+n-\nu+\gamma_1\right)a^{\gamma_2} - \left(1+n-\nu+\gamma_2\right)a^{\gamma_1}},$$
$$B = B_e = \frac{\tau a^{\gamma_1}}{\left(1+n-\nu+\gamma_1\right)a^{\gamma_2} - \left(1+n-\nu+\gamma_2\right)a^{\gamma_1}}. \tag{17}$$

Substituting (14) at $\rho = a$ into (2) and using (17) it is possible to find the value of τ corresponding to the initiation of the plastic zone as

$$\tau_e = \frac{a^{\gamma_2}\left(1+\gamma_1+n-\nu\right) - a^{\gamma_1}\left(1+\gamma_2+n-\nu\right)}{a^{\gamma_1}a^{\gamma_2}\left(\gamma_1-\gamma_2\right)} \tag{18}$$

Then, substituting (17) and (18) into (14) yields the following value of the stress σ_θ at $\rho = a$ and $\tau = \tau_e$

$$\sigma_\theta = -\sigma_Y\,. \tag{19}$$

2.3 Elastic/plastic stress solution

As for the elastic/plastic stress solution, the yield criterion (2) is satisfied by the following substitution

$$\frac{\sigma_r}{\sigma_Y} = -\frac{2\sin\psi}{\sqrt{3}}, \quad \frac{\sigma_\theta}{\sigma_Y} = -\frac{\sin\psi}{\sqrt{3}} - \cos\psi \tag{20}$$

where ψ is a new unknown function of *p* and ρ. The plastic zone propagates from the hole toward to outer rim. Therefore, the stresses given in (20) must satisfy the boundary condition (12), and substituting (20) into (11) gives

$$2\rho\cos\psi\frac{\partial\psi}{\partial\rho} - \sqrt{3}\cos\psi + \left(1+2n\right)\sin\psi = 0\,. \tag{21}$$

Using (12) and (19) it is possible to find from (20) that $\psi = 0$ at $\rho = a$. Solving (21) with the use of this boundary condition results in

$$\frac{\rho}{a}=\exp\left[\frac{\sqrt{3}\psi}{2\left(1+n+n^2\right)}\right]\left[\cos\psi-\frac{\left(1+2n\right)}{\sqrt{3}}\sin\psi\right]^{\beta},$$
$$\beta=-\frac{1+2n}{2\left(1+n+n^2\right)} \tag{22}$$

Let ψ_c be the value of ψ at the elastic/plastic boundary, $\rho=\rho_c$. Then, it follows from (22) that

$$\frac{\rho_c}{a}=\exp\left[\frac{\sqrt{3}\psi_c}{2\left(1+n+n^2\right)}\right]\left[\cos\psi_c-\frac{\left(1+2n\right)}{\sqrt{3}}\sin\psi_c\right]^{\beta}. \tag{23}$$

Both σ_r and σ_θ are continuous across the elastic/plastic boundary. The distribution of the stresses in the elastic zone is given by (14). Then, combining (14) and (20) results in

$$\begin{aligned} &Ar_c^{g_1}+Br_c^{g_2}=-\frac{2\sin\gamma_c}{\sqrt{3}},\\ &A\left(1+n+g_1\right)r_c^{g_1}+B\left(1+n+g_2\right)r_c^{g_2}=-\frac{\sin\gamma_c}{\sqrt{3}}-\cos\gamma_c. \end{aligned} \tag{24}$$

These equations along with (23) are used to express *A* and *B* in terms of ψ_c as

$$\begin{aligned} A&=\frac{1}{\sqrt{3}}\left[\frac{\sqrt{3}\cos\psi_c-\left(1+2n+2\gamma_2\right)\sin\psi_c}{\gamma_2-\gamma_1}\right]\rho_c^{-\gamma_1},\\ B&=-\frac{1}{\sqrt{3}}\left[\frac{\sqrt{3}\cos\psi_c-\left(1+2n+2\gamma_1\right)\sin\psi_c}{\gamma_2-\gamma_1}\right]\rho_c^{-\gamma_2} \end{aligned} \tag{25}$$

Here ρ_c should be eliminated by means of (23). Combining the boundary condition (13) and the solution (15) for ε_θ gives

$$\tau=-\left(1+n-\nu+\gamma_1\right)A-\left(1+n-\nu+\gamma_2\right)B. \tag{26}$$

Eliminating *A* and *B* in (26) by means of (25) leads to

$$\begin{aligned} t=&-\frac{\left(1+n-n+g_1\right)}{\sqrt{3}}\left[\frac{\sqrt{3}\cos\gamma_c-\left(1+2n+2g_2\right)\sin\gamma_c}{g_2-g_1}\right]r_c^{-g_1}+\\ &+\frac{\left(1+n-n+g_2\right)}{\sqrt{3}}\left[\frac{\sqrt{3}\cos\gamma_c-\left(1+2n+2g_1\right)\sin\gamma_c}{g_2-g_1}\right]r_c^{-g_2} \end{aligned} \tag{27}$$

The entire disc becomes plastic when $\rho_c=1$. The corresponding values of ψ_c and τ are denoted by ψ_p and τ_p, respectively. The equation for ψ_p follows from (23) as

$$1=a\exp\left[\frac{\sqrt{3}\psi_p}{2\left(1+n+n^2\right)}\right]\left[\cos\psi_p-\frac{\left(1+2n\right)}{\sqrt{3}}\sin\psi_p\right]^{\beta}. \tag{28}$$

The value of τ_p is determined from (27) at $\psi_c=\psi_p$ as

$$\tau_p = -\frac{(1+n-\nu+\gamma_1)}{\sqrt{3}}\left[\frac{\sqrt{3}\cos\psi_p - (1+2n+2\gamma_2)\sin\psi_p}{\gamma_2-\gamma_1}\right] + \\ + \frac{(1+n-\nu+\gamma_2)}{\sqrt{3}}\left[\frac{\sqrt{3}\cos\psi_p - (1+2n+2\gamma_1)\sin\psi_p}{\gamma_2-\gamma_1}\right]. \quad (29)$$

The normalized temperature is defined as follows to measure the difference between elastic and plastic temperatures.

$$dt = \frac{T_p - T_e}{T_e}. \quad (30)$$

The normalized temperature indicates the range of temperature for the disc to go from purely elastic deformation ($T = T_e$) up to plastic collapse ($T = T_p$).

2.4 Elastic/plastic strain solution at $\tau_e \le \tau \le \tau_p$ *(or* $0 \ge \psi_c \ge \psi_p$*)*

Consider the plastic zone. Eliminating λ in (8) and using (20) yield

$$2\cos\psi\zeta_r^p = \left(\sqrt{3}\sin\psi - \cos\psi\right)\zeta_\theta^p, \quad 2\cos\psi\zeta_z^p = -\left(\cos\psi + \sqrt{3}\sin\psi\right)\zeta_\theta^p. \quad (31)$$

It is evident from (22) that ψ is independent of p . Therefore, taking into account the definition for ζ_r^p , ζ_θ^p and ζ_z^p introduced in (7) equations (31) can be immediately integrated with respect to p to give

$$2\cos\psi\varepsilon_r^p = \left(\sqrt{3}\sin\psi - \cos\psi\right)\varepsilon_\theta^p, \quad 2\cos\psi\varepsilon_z^p = -\left(\cos\psi + \sqrt{3}\sin\psi\right)\varepsilon_\theta^p. \quad (32)$$

This solution satisfies the condition that all the plastic strains vanish simultaneously. In particular, it is evident that the condition that all the plastic strains vanish at the elastic-plastic boundary is equivalent to the condition that one of these strains vanishes. It is seen from (31) and (32) that there is no difference between the deformation and flow theories of plasticity in the case under consideration. It follows from (6) that the equation of strain compatibility is $\rho\partial\varepsilon_\theta/\partial\rho = \varepsilon_r - \varepsilon_\theta$. Using (4) and (5) this equation transforms to

$$\rho\frac{\partial\varepsilon_\theta^e}{\partial\rho} + \rho\frac{\partial\varepsilon_\theta^p}{\partial\rho} = \varepsilon_r^e + \varepsilon_r^p - \varepsilon_\theta^e - \varepsilon_\theta^p. \quad (33)$$

Substituting (20) into (3) gives

$$\varepsilon_r^e = k\left[\nu\cos\psi - \frac{(2-\nu)}{\sqrt{3}}\sin\psi\right], \quad \varepsilon_\theta^e = -k\left[\cos\psi + \frac{(1-2\nu)}{\sqrt{3}}\sin\psi\right], \\ \varepsilon_z^e = k\nu\left(\cos\psi + \sqrt{3}\sin\psi\right). \quad (34)$$

Substituting (32) and (34) into (33) and replacing differentiation with respect to ρ with differentiation with respect to ψ by means of (21) yield

$$\frac{\partial \varepsilon_\theta^p}{\partial \psi} - \frac{\sqrt{3}\left(\sin\psi - \sqrt{3}\cos\psi\right)}{\sqrt{3}\cos\psi - (1+2n)\sin\psi}\varepsilon_\theta^p = k\Lambda(\psi),$$
$$\Lambda(\psi) = \frac{2(1+\nu)\cos\psi\left(\sqrt{3}\cos\psi - \sin\psi\right)}{\sqrt{3}\left[\sqrt{3}\cos\psi - (1+2n)\sin\psi\right]} + \frac{(1-2\nu)}{\sqrt{3}}\cos\psi - \sin\psi \tag{35}$$

The solution of this equation satisfying the boundary condition $\varepsilon_\theta^p = 0$ for $\psi = \psi_c$ is

$$\varepsilon_\theta^p = kV(\psi,\psi_c)U(\psi,\psi_c),$$
$$V(\psi,\psi_c) = \exp\left[-\frac{\sqrt{3}}{2}\frac{(2+n)}{(1+n+n^2)}(\psi-\psi_c)\right]\left[\frac{\sqrt{3}\cos\psi - (1+2n)\sin\psi}{\sqrt{3}\cos\psi_c - (1+2n)\sin\psi_c}\right]^\mu,$$
$$U(\psi,\psi_c) = \int_{\psi_c}^{\psi}\Lambda(x)\exp\left[\frac{\sqrt{3}}{2}\frac{(2+n)}{(1+n+n^2)}(x-\psi_c)\right]\left[\frac{\sqrt{3}\cos\psi_c - (1+2n)\sin\psi_c}{\sqrt{3}\cos x - (1+2n)\sin x}\right]^\mu dx, \tag{36}$$
$$\mu = \frac{3n}{2(1+n+n^2)}$$

The other plastic strain components may be determined from (32) and (36). Using (16) and (27), equation (4) can be rewritten in the form

$$\varepsilon_r^T = \varepsilon_\theta^T = \varepsilon_z^T = -k(1+n-\nu+\gamma_1)\rho_c^{-\gamma_1}\left[\cos\psi_c - \frac{\sin\psi_c}{\sqrt{3}}(2\gamma_2+1+2n)\right](\gamma_2-\gamma_1)^{-1} -$$
$$-k(1+n-\nu+\gamma_2)\rho_c^{-\gamma_2}\left[-\cos\psi_c + \frac{\sin\psi_c}{\sqrt{3}}(2\gamma_1+1+2n)\right](\gamma_2-\gamma_1)^{-1}. \tag{37}$$

It is seen from (5), (34), (36) and (37) that all the strain components are proportional to *k*. Thus, simple scaling of a single solution for a disc of given *a* – value and Poisson's ratio supplies the solutions for similar discs of material with the same Poisson's ratio but any temperature-dependent yield stress and Young's modulus. Also, the value of γ is not involved in the solution in terms of τ. However, both *k* and γ are necessary to find the physical temperature according to (9) and (16). The solution found provides the radial distribution of strains in the plastic zone in parametric form with ψ being the parameter varying in the range $0 \le \psi \le \psi_c$. In particular, the total strains are found from (5), (32), (34), (36), and (37). In the elastic zone, the total strains are given by (15) where *A* and *B* should be eliminated by means of (25).

2.5 Elastic/plastic strain solution at $\tau_p \le \tau$.

Equations (22), (32), (34) and (35) are valid in the range $a \le \rho \le 1$. Using (16) equation (4) can be rewritten in the form

$$\varepsilon_r^T = \varepsilon_\theta^T = \varepsilon_z^T = k\tau. \tag{38}$$

Let ψ_b be the value of ψ at $\rho = 1$. Then, substituting (34) and (38) into (5) and the resulting expression for ε_θ into the boundary condition (13) give

$$\varepsilon_\theta^p = k\left[\cos\psi_b + \frac{(1-2\nu)}{\sqrt{3}}\sin\psi_b\right] - k\tau \tag{39}$$

at $\rho = 1$ (or $\psi = \psi_b$). Moreover, it follows from (22) that

$$\frac{1}{a} = \exp\left[\frac{\sqrt{3}\psi_b}{2\left(1+n+n^2\right)}\right]\left[\frac{\sqrt{3}\cos\psi_b - (1+2n)\sin\psi_b}{\sqrt{3}}\right]^\beta. \tag{40}$$

Thus the value of ψ_b does not change with temperature at $\tau_p \le \tau$. Therefore, $\psi_b = \psi_p$. The solution of equation (35) satisfying the boundary condition (39) is

$$\frac{\varepsilon_\theta^p}{k} = V\left(\psi, \psi_p\right)\left[U\left(\psi, \psi_p\right) + \cos\psi_p + \frac{(1-2\nu)}{\sqrt{3}}\sin\psi_p - \tau\right]. \tag{41}$$

The other plastic strain components are determined from (32) and (41). Thus the radial distribution of the plastic strains has been determined in parametric form with ψ being the parameter varying in the range $0 \le \psi \le \psi_p$. Having the solution for the plastic strains the total strains are immediately found from (5), (32), (34), (38), and (41).

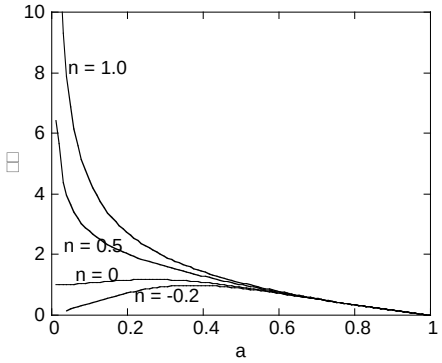

Figure 3. Normalized temperature, versus normalized radius, *a*, for various hyperbolic profile *n*, calculated from Eq. (30).

3. EXAMPLES AND DISCUSSION

In our numerical examples of the above derived analytical results, the high-strength low-alloy steel is chosen, and its time-dependent material functions $f_E(T)$, $f_\gamma(T)$, and $f_\sigma(T)$ in the range $0 \le T < 400^0 C$ are as follows.

$$f_E(T) = 1 + \frac{T}{2000\ln(T/1100)}, \quad f_\sigma(T) = 1 + \frac{T}{600\ln(T/1630)}, \tag{42}$$
$$f_\gamma(T) = 1 + 2.56\times10^{-4}T + 2.14\times10^{-7}T^2$$

where the temperature difference *T* is in ˚*C* and the initial temperature is 20˚*C* (Argeso and Eraslan 2008). In other words, when T = 0, the temperature is the initial temperature. In addition, $E_0 = 200GPa$, $\sigma_0 = 410MPa$, $\nu = 0.3$, and $\gamma_0 = 11.7\times10^{-6}$ per ˚*C*. We remark that temperature-dependent material properties are assumed throughout the calculated examples, except stated otherwise.

Using these functions the temperature variation, Figure 3 shows the normalized temperature versus normalized radius *a*, as calculated from (30), for various hyperbolic profile *n*. The physical meaning of the normalized temperature is the temperature range of the disc will experience above Te (upper temperature limit for purely elastic deformation) but smaller than Tp (plastic collapse, i.e. plastic deformation everywhere in the disc). It can be seen that for large hole size (a greater than about 0.6), linearly decreases as *a* increases, regardless of the *n* value. In other words, thickness variations do not play a role for discs with a large hole in the middle. For small holes, *a* less than about 0.4, positive *n* values will lead to large , while negative *n* values reduce the temperature range. Physically, negative *n* values result in larger thickness around the hole, and once it is in plastic zone due to temperature increase, the whole disc will go into plastic deformation with a slightly additional temperature increase.

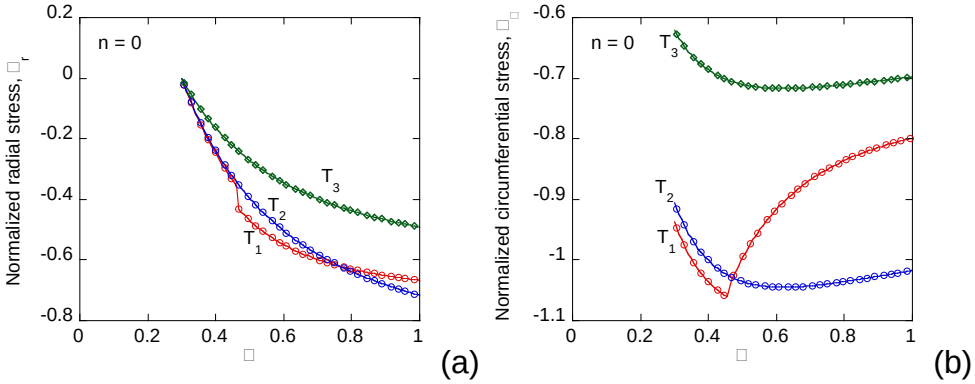

Figure 4. Stress distribution along the radius for the n = 0 case,. (a) Radial stress, and (b) circumferential stress.

Figures 4 and 5, respectively, show the stress and strain distribution for *n = 0* and *a = 0.3* to delineate how the stress and strain vary along the radial direction. Three temperatures are adopted, T_1 = 104.26, T_2 = 139.95 and T_3 = 350. For n = 0, the Te and Tp are 68.57 and 139.95, respectively. Hence, when T = T_2, plastic collapse occurs. The radial and circumferential stress are plotted in Figure 4 (a) and (b), respective. It can be seen that both stresses are compressive. For radial stress, as increases, the stress magnitude increases, i.e. the radial stress becomes more negative. However, this monotonicity does not occur for the circumferential stress. When T = T_1, part of the disc is still in the purely elastic state, and the elastic-plastic boundary is at about = 0.45, where radial stress shows a jump and circumferential stress becomes non-differentiable. In addition, higher temperatures result in higher circumferential stress, but radial stress reduces for large T.

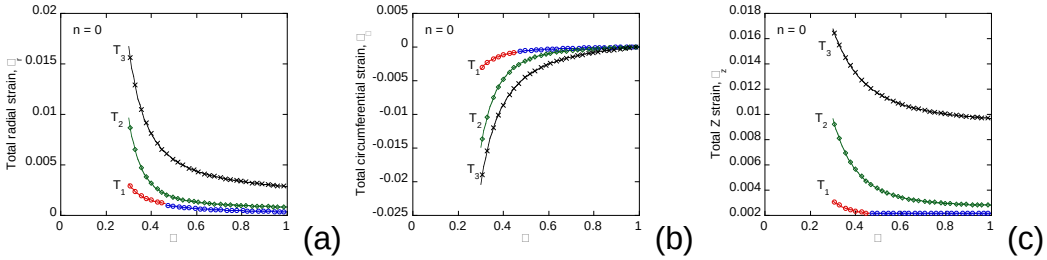

Figure 5. Strain distribution along the radius for the n = 0 case,. (a) Radial strain, (b) circumferential strain and (c) Z strain, the strain along the thickness direction.

The total radial strain, circumferential strain and Z strain are shown in Figure 5 (a), (b) and (c), respectively, for the n = 0 case. It can be seen that the total circumferential strain reaches zero at = 1, as expected. Larger temperatures result in larger magnitudes in all strain components.

In order to examine the effects of the thickness variations with the derived analytical solutions here, Figure 6 shows the comparisons on circumferential strain for two different temperatures, namely T = 106.3 and T = 350. Three n values are calculated, n_1 = -0.2, n_2 = 0 and n_3 = 0.5. It is noted that the plastic collapse temperature Tp depends on the n values. Hence, the three n's lead to the following three plastic collapse temperatures 132.49, 139.95 and 150.31 for n = -0.2, 0 and 0.5, respectively. The corresponding Te's are 71.69, 68.57, 62.28 also for n = -0.2, 0 and 0.5, respectively. In Figure 6 (a), T > Te, but less than Tp for all n's. It can be seen that as n increases from negative values to positive values, the circumferential strain becomes more negative. In other words, the strain for n > 0 is more negative, i.e. larger, than the strain for n = 0. However, the strain for n < 0 is less negative, i.e. smaller than the strain for n = 0. When comparing Figure 6 (a) and (b), this relationship is reversed. In other words, when T = 350, which makes the disc plastically deformed everywhere, n < 0 results in an increase in strain.

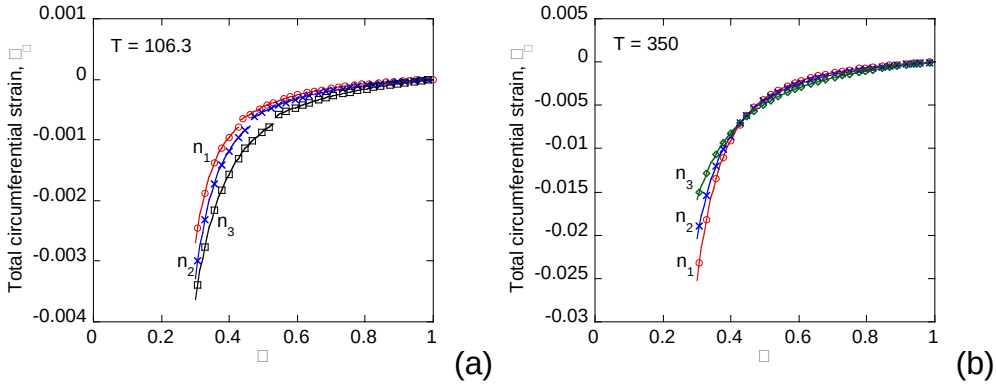

Figure 6. Effects of the thickness variations for (a) T = 106.3 < Tp, and (b) T = 350 > Tp.

As for the effects of the temperature dependent material properties, Figure 7 (a) and (b) show comparisons on the circumferential strain for n = 0 and n = 0.5, respectively, at the three temperatures. It can be seen that when n = 0, the disc has uniform thickness, the effects of the temperature dependent material properties are

minor. However, the combined effects of the thickness variations and temperature-dependent material properties show stronger effects, particularly at high temperatures, i.e. $T = T_3$. Therefore, in real-world applications, the considerations of temperature-dependent material properties are crucial when thickness variations are present.

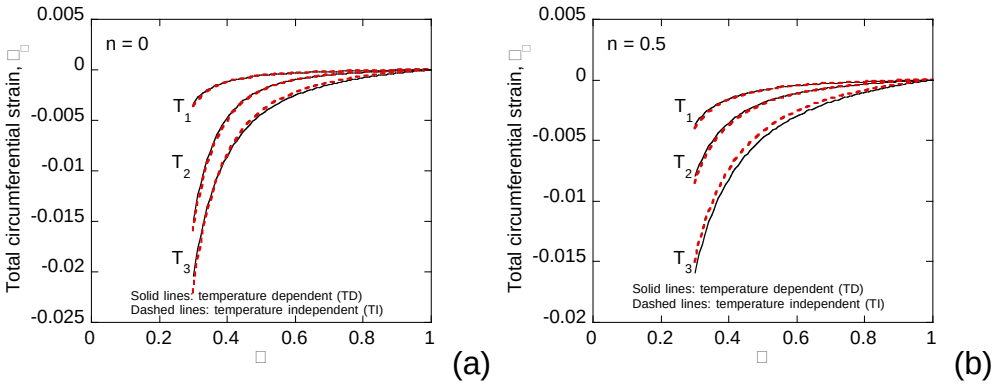

Figure 7. Effects of the temperature-dependent material properties for (a) n = 0 and (b) n = 0.5.

4. CONCLUSIONS

Analytical solutions, in the purely elastic, elastic-plastic and fully plastic situation, of the hollow disk with hyperbolic thickness profile under uniform temperature field have been obtained, including temperature dependent material properties. The Poisson's ratio of the material is assumed to be temperature independent. It is found that the thickness variations, controlled by the *n* value, have strong effects on the stress and strain distribution, as well as the normalized temperature difference . Furthermore, it is shown that the combined effects of thickness variations and the temperature-dependent material properties may cause notable deviations from simple analysis that does not include the two effects.

ACKNOWLEDGEMENTS

One of the authors, YCW, is grateful for research grants from Taiwan NSC 101-2221-E-006-206. The research described in this paper has been partly supported by the grants NSC-99-2218-E-194-003-MY3 and NSH-3842.2012.1. A part of this work was done while Sergei Alexandrov was with National Chung Cheng University (Taiwan) as a research scholar under the recruitment program supported by the National Science Council of Taiwan (contract 99-2811-E-194-009).

REFERENCES

Alujevic, A., Les, P. and Zupec, J. (1993), "Thermal yield of a rotating hyperbolic disk," *Zeitschrift fur Angewandte Mathematik und Mechanik (ZAMM)*, **73**, T283–T287.

Alexandrov, S., Jeng, Y.-R., and Lyamina, E. (2012), "Influence of pressure-dependency of the yield criterion and temperature on residual stresses and strains in a thin disk," *Struct. Eng. Mech.*, **44**, 289–303.

Alexandrova, N. and Alexandrov, S. (2004), “Elastic-plastic stress distribution in a plastically anisotropic rotating disk,” *Trans. ASME J. Appl. Mech.*, **71**, 427–429.

Argeso, H. and Eraslan, A.N. (2008), “On the use of temperature-dependent physical properties in thermomechanical calculations for solid and hollow cylinders,” *Int. J. Therm. Sci.*, **47**, 136–146.

Eraslan, A.N. (2002), “Von Mises yield criterion and nonlinearly hardening variable thickness rotating annular disks with rigid inclusion,” *Mech. Res. Commun.*, **29**, 339–350.

Eraslan, A.N. (2003), “Elastic-plastic deformations of rotating variable thickness annular disks with free, pressurized and radially constrained boundary conditions,” *Int. J. Mech. Sci.*, **45**(4), 643–667.

Eraslan A.N., Orcan Y. and Guven, U. (2005), “Elastoplastic analysis of nonlinearly hardening variable thickness annular disks under external pressure,” *Mech. Res. Commun.*, **32**(3), 306–315.

Eraslan, A.N. and Orcan, Y. (2002), “On the rotating elastic-plastic solid disks of variable thickness having concave profiles,” *Int. J. Mech. Sci.*, **44**(7), 1445–1466.

Gamer, U. (1984), “Elastic-plastic deformation of the rotating solid disk,” *Archive Appl. Mech. (Ingenieur Archiv)*, **54**(5), 345–354.

Guven, U. (1998), “Elastic-plastic stress distribution in a rotating hyperbolic disk with rigid inclusion,” *Int. J. Mech. Sci.*, **40**(1), 97–109.

Horstemeyer, M.F. and Bammann, D.J. (2010), “Historical review of internal state variable theory for inelasticity,” *International Journal of Plasticity*, **26**, 1310–1334.

Lenard, J. and Haddow, J.B. (1972), “Plastic collapse speeds for rotating cylinders,” *Int J Mech Sci.*, **14**(5), 285–292.

Noda., N. (1991). “Thermal stresses in materials with temperature-dependent properties,” *Appl. Mech. Rev.*, **44**, 383–397.

Rees, D.W.A. (1999), “Elastic-plastic stresses in rotating disks by von Mises and Tresca,” *Zeitschrift fur Angewandte Mathematik und Mechanik (ZAMM)*, **79**(4), 281–288.

Thompson, A.S. and Lester, P.A. (1946), “Stresses in rotating disks at high temperatures,” *J. Appl. Mech.*, **13**, A45–A52.

Vivio, F. and Vullo, L. (2010), “Elastic-plastic analysis of rotating disks having non-linearly variable thickness: residual stresses by overspeeding and service stress state reduction,” *Ann. Solid Struct. Mech.*, **1**, 87–102.

Withers., P.J. (2007). “Residual stress and its role in failure,” *Rep. Prog. Phys.*, **70**, 2211–2264.

You L.H. and Zhang, J.J. (1999), “Elastic-plastic stresses in a rotating solid disk,” *Int. J. Mech. Sci.*, **41**(3), 269–282.

Zimmerman, R.W. and Lutz, M.P. (1999), “Thermal stresses and thermal expansion in a uniformly heated functionally graded cylinder,” *J. Therm. Stresses*, **22**, 177–188.